

EFFECT OF LINK BEAM LENGTH OF THE ECCENTRIC BRACING SYSTEM ON SEISMIC REHABILITATION OF WEAK REINFORCED CONCRETE FRAMES

Touraj NIKNAM¹, Hamid SABERI¹, Vahid SABERI¹, Abbasali SADEGHI²,
Ehsan NOROOZINEJAD FARSANGI^{3*}

¹ Department of Civil Engineering, Eyvanekey University, Semnan, Iran

² Department of Civil Engineering, Mashhad Branch, Islamic Azad University,
Mashhad, Iran

³ Faculty of Civil and Surveying Engineering, Graduate University of Advanced
Technology, Kerman, Iran

Abstract

In this study, A reinforced concrete (RC) reference specimen with compressive strength of 250 kg/cm^2 and the weak RC specimen for seismic rehabilitation with compressive strength of 150 kg/cm^2 were examined in two types of structures with 6 and 12-stories. The link beam lengths of 50, 80, and 100 cm have been used in 6 and 12-stories prototypes under the effect of 7 earthquake records. The nonlinear dynamic analyses are performed. Then, The behavior of the link beam depends on its length. For short link beam lengths, shear behavior is serious, then for medium lengths, shear-flexural behavior is important, and finally, long lengths will have flexural behavior for the beam. In eccentrically braced frames, the details of the link beam and the fit of the other members must be done in such a way as to ensure its proper ductility. According to the obtained results, the performance of short link beams is much better than long link beams, and short link beams provide more energy dissipation and, at the same time, more ductility. Therefore, in the design of the link beam, mainly the shear of the link beam is considered as a ductile component. The axial force in the link beam, which is due to the application of lateral load to the structure,

* Corresponding author: Ehsan Noroozinejad Farsangi, Assistant Professor, Faculty of Civil and Surveying Engineering, Graduate University of Advanced Technology, P.O. Box 117-76315, Kerman 7631818356, Iran. Email: noroozinejad@kgut.ac.ir

reduces both the bending capacity and the inelastic deformation capacity of the link beam, so it can be explained that in steel eccentric braces, the link beam is symmetrical between the two main components of the brace and it can affect the strength of the structure against lateral loads.

Keywords: link beam length, eccentric brace, seismic rehabilitation, weak reinforced concrete (*RC*) frame

1. INTRODUCTION

In some buildings, the stiffness and strength of the building are insufficient due to a variety of factors such as a change in design guidelines, a variation in the occupancy type of the building, the addition of new stories to the building, or a lack of adequate strength in the concrete, and thus retrofitting the building is unavoidable. These buildings must be modified in such a way that they are suited to the new conditions while also meeting the guidelines' criteria. Various seismic characteristics, such as the strength reduction factor, over-strength factor, ductility, period, and so on, must be understood before retrofitting a structure. These characteristics are provided for typical earthquake resistant structures such as concrete and steel moment-resisting frames, *X* braced frames, and so on by various standards such as *ASCE 7-05* [1]. When a reinforced concrete (*RC*) moment-resisting frame is strengthened with concentric or eccentric braces, the seismic characteristics of the structure, such as the period and the strength reduction factor, and therefore the earthquake's base shear altered. As a result, in order to retrofit the building, the characteristics of the new compound system must be known. The seismic characteristics of these sorts of compound frames have been barely discussed in design standards, and retrofitting these buildings is more reliant on engineering judgment and nonlinear analysis. It should be noted that nonlinear finite element studies are challenging and time consuming because to the highly complicated behavior of concrete, particularly the contact components between steel and concrete. Numerous research on retrofitting *RC* buildings with steel elements have been undertaken in recent years, some of which will be discussed in the followings. Del Valle completed the seismic retrofit of a 12-story *RC* structure in Mexico in 1980 [2]. Miranda and Bertero evaluated the effectiveness of post-tension bracing in an attempt to enhance the responsiveness of low-rise school buildings in Mexico in 1990 [3]. It should be noted that the study was conducted on Mexico's western coast, where soft soil is prevalent. Badoux and Jirsa examined the usage of steel bracing in improving the seismic strength of *RC* frames analytically [4]. In that work, the inelastic buckling of the braces was examined, and the method for modifying the beams of the braced frame was defined. Bush et al. studied the experimental retrofitting of a *RC* frame with steel bracing [5]. The structure under consideration was a two bay-three story

frame with a scale of a 2:3 scale that was subjected to cyclic loading. They improved the in-plane shear strength of the frame significantly and discovered that the increased shear capacity of the retrofitted frame is dependent on the capacity of the braces, how they are attached to the frame, and the shear strength of the column. Rodriguez and Park examined the studies on retrofitting *RC* structures, especially *RC* column rehabilitation [6]. They determined that utilizing steel bracing is one of the most efficient ways to retrofit *RC* frames after evaluating various retrofitting methods. Pincheira conducted a series of experiments on retrofitting of *RC* frames and compiled the findings of prior investigations [7]. The post-tensioned brace and the *X* brace were among the methods explored for retrofitting *RC* structures, and the displacement control technique was developed for designing these structures. Lobo et al. investigated the impact of Visco-elastic bracing on *RC* structure response [8]. They demonstrated that, while this bracing system can preserve the structure in the elastic phase, it may also serve as an energy dissipater. As a result, it has the potential to slow the pace at which fractures expand in an *RC* structure. Nateghi published research on the use of steel bracing to reinforce an eight-story residential building [9]. The paper discusses retrofitting methods as well as steps done to fortify the structure against lateral and vertical loads. Pincheira and Jirsa used nonlinear static and dynamic calculations to examine the seismic performance of various retrofitting solutions for inflexible *RC* frames [10]. The chosen structures featured the reinforcing elements seen in older frames, and the retrofitting designs included the installation of post-tensioned braces, steel braces, or *RC* filling walls. The findings demonstrated that there is no one answer and that several retrofitting approaches may be used to attain a suitable performance. Masri and Goel presented their findings on the use of ductile steel bracing to retrofit *RC* moment-resistant frames with flat slabs [11]. They ran an experiment on a two-bay, two-story *RC* frame with a 1:3 scale. The performance of the modified frame was noticeably superior to that of the original frame. Ghobarah and Elfath investigated the use of an eccentric steel bracing in the retrofitting of *RC* frames [12]. The performance of modified frames was evaluated in that investigation utilizing nonlinear static and time historical dynamic assessments based on narrative drift and the damage index. Youssef et al. investigated the seismic performance of *RC* frames modified with concentric steel bracing [13]. Two cyclic loading experiments were performed on an *RC* moment-resisting frame and a braced *RC* frame. The study's findings revealed that the braced frame has more strength than the moment-resisting frame and exhibits appropriate ductility. Mazzolani investigated some retrofitting methods, including adding eccentric braces, aluminum shear panels and buckling-restrained braces (*BRBs*) [14]. He showed that retrofitting with eccentric braces with a vertical link yields the highest increase in load carrying capacity, about 5.5 to 8 times the base values of the retrofitted structure. These

improvements in strength are about 4.25 times for the *BRB* and approximately 4 times for the aluminum shear panel. Sadeghi et al. assessed the reliability of steel structures under severe vehicle impact loadings by using Monte Carlo Simulation (*MCS*). To reduce computational costs, meta-model methods are employed, and their efficiency is assessed. The new results showed that Kriging could predict the failure probability of steel frame with high accuracy [15]. Furthermore, Sadeghi et al. evaluated the collapse capacity and endurance duration of steel structures with a corner damaged column exposed to vehicle impact under seismic ground motions [16].

It is clear that significant study has been conducted on strengthening *RC* frames with steel components. Although all studies agree on enhancing the stiffness, strength, and energy dissipation of *RC* frames, no similar study has been done to adequately assess the impact of steel eccentric bracing with different link beam lengths on the seismic characteristics of *RC* moment resistant frames. The primary objective of this study is to conduct a numerical evaluation of the impacts of the steel eccentric bracing with different link beam lengths in retrofitting of *RC* frames and compare their seismic characteristics. In the following, the performance of *RC* frames with 6 and 12-stories are assessed under 7 near-fault records by using nonlinear dynamic time history analysis.

2. MODELING PROCEDURE

2.1. Modeling verification

Initially, the specimen of a reinforced concrete frame with a brace, which was investigated in the laboratory by Tahamouli Roudsari et al., [17] was simulated by finite element software. The purpose of this simulation is to validate the numerical model created to investigate the parameters affecting the link beam behavior. The *ABAQUS* software is used in this research to numerically simulate a reinforced concrete frame with a brace. The dimensions and sizes of the link components are exactly the same as the specimen of the *RC* frame with a brace made in the laboratory. The size of the frame was 1:3, with beam and column lengths of 1.45 and 1 m, respectively. The size of the beam and column sections were decided to be 150 mm. The frame's embedded reinforcement was done in such a way that the criteria of the intermediate moment-resisting frame could be satisfied. The primary steel bars and stirrups were 414 and 8@45 mm for the columns and 410 and 8@45 mm for the beam (the "8@45" phrase implies that one rebar with a diameter of 8 mm is used every 45 mm). In addition, 414 stirrups were put at the top of the frame and 314 stirrups were set at the bottom with 8@80 mm stirrups. While the frames' concrete was being poured, certain specimens were removed to evaluate the concrete's compressive strength. The axial compression test was performed on these specimens after 72 days, concurrently with the testing

of the frames, and an average strength of 35.2 MPa was achieved. All components of the specimen are constructed with *C3D8R* elements. The use of this type of element, in accordance with the simulation needs of this type of link beam, is one of the pasty behavior of materials and contact tensions. Specimen components of *RC* frame with bracing include concrete frame, a brace have finer grid, and this is due to more focus on the behavior of the link components and also the two surfaces in contact with each other. Figure 1 depicts the entire experiment setup of eccentric braced placed in *RC* frame. The frame has been vertically connected to a very robust chassis on the lab floor using twelve pre-stressed $26 \text{ mm } 12.9$ screws in line with *ISO* standard [18]. The complete setup of the experiment is shown in Figure 1. It can be seen that the frame has been vertically fixed to a very strong chassis on the floor of the lab using twelve pre-stressed $26 \text{ mm } 12.9$ screws in accordance with the *ISO* standard. To prevent slippage between the structure's base and the chassis, two L-shaped yellow back-stays were placed on opposite sides of the foundation. The stress was provided as tension and compression in a quasistatic manner utilizing a 1000 kN hydraulic actuator. The actuator's maximum displacement capacity was 150 mm and the loading type were both displacement control. One end of the actuator was fastened to the top cap of the frame, while the other end was linked to the response frame as a solid connection. The utilized material parameters for retrofitting specimens 2 to 8 based on the tensile test are presented in reference [17]. Cyclic loading was applied to the specimens in line with the *ACI Committee 374.1-05* [19] loading technique. The loading was sustained until failure occurred and a decrease in the hysteresis diagram was seen. The drift values were multiplied by the frame height (the distance between the centre of the beam and the top of the foundation), which was 1000 mm , and then applied as displacement to the top of the frame. Lateral bracings were added on both sides of the frame to prevent lateral movement. A 32-channel data-logger was used to record the data. The displacements were delivered to the beam very slowly, and the data were collected every 10 seconds. A Linear Variable Differential Transformer (*LVDT*) with a precision of 0.01 mm and a maximum displacement capacity of 200 mm was used to measure the displacement at the top of the frame. A linear potentiometer with a precision of 0.1 mm was also used to monitor displacement at the middle of the column.

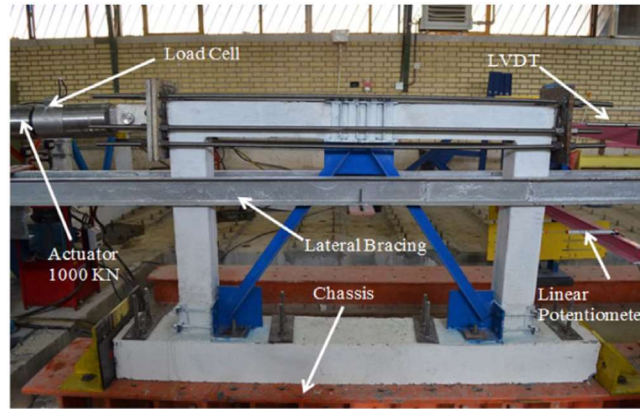


Fig. 1. The configuration of experimental specimen [17]

In the step module, based on Fig. 6 specify the type of analysis or analyses that you want to perform by *ABAQUS* solvers in the form of step definition. In fact, each individual analysis is done in the form of a step. When you create a step, you see that the step called the initial step has already been created. The software always considers this step as the first step of any analysis. In this step, the initial conditions of the problem, such as initial temperature, initial velocity or initial stresses, if non-zero, must be defined. Due to the complexity of the model and having many contacts, Dynamic, explicit or quasi-static has been used to slow down the analysis speed. The finite element model is presented based on Fig. 2. Also, the loading protocol is applied based on Fig. 3.

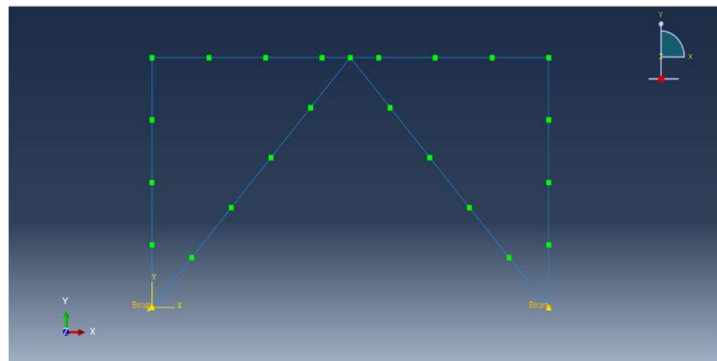


Fig. 2. The modeled experimental specimen

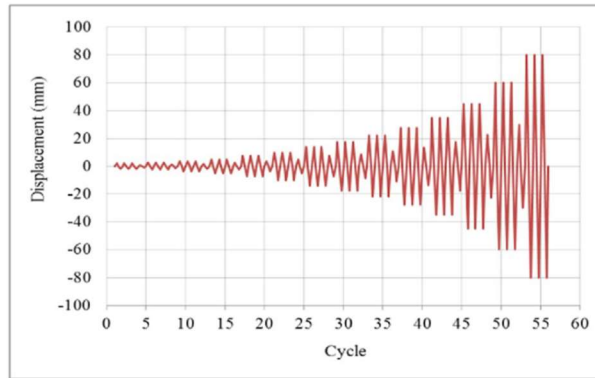


Fig. 3. The loading protocol

By submitting the defined job, the solution process begins, so to validate the designed model, the laboratory specimen and the specimen made in the software are compared, as well as the color contour of the displacement, Von-Mises stress and base shear counters based on Figs 4 to 6, respectively.

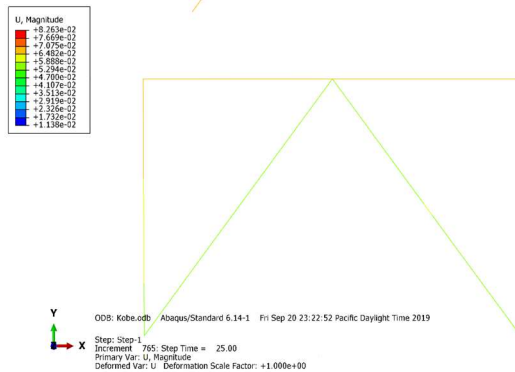


Fig. 4. The maximum displacement counter of the modeled specimen

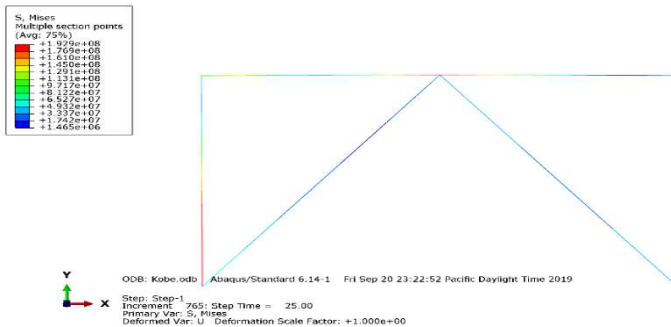


Fig. 5. The maximum Von Mises stress counter of the modeled specimen

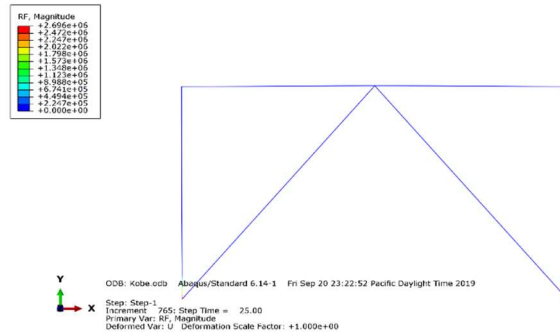


Fig. 6. The base shear counter of the modeled specimen

The force-displacement diagram of the model under considerations include a RC frame reinforced with a brace. We compared both the experimental and the analytical diagrams with each other based on Fig. 7. The error rate of experimental and finite element models is insignificant. This value is equal to a maximum 5%. Therefore, the procedure of modeling is valid.

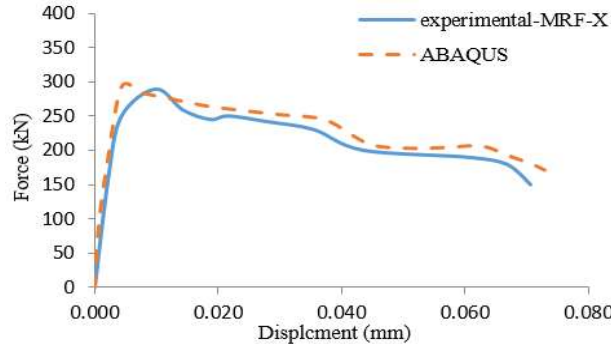


Fig. 7. The results of experimental and finite element models

2.2. The studied models

In order to achieve the objectives of this study, we model 6 and 12-stories with a combined system of moment frame and an eccentric brace. The two frames of 6 and 12-stories have three openings with a width of 5 m, the height of each floor 3 meters and in an eccentric bracing system, the length of link beam 50, 80 and 100 cm is considered in ABAQUS software by linear beam element model (two-dimensional) and acceleration loading is applied to the base of the frame. 7 earthquake records are studied in this research. Also, the combined effect of moment frame and an eccentric bracing is attributed to the rate of deformation and the amount of deformation of the link beam beams. The dynamic behavior of the structure against earthquake acceleration has been investigated. Two frames of 6 and 12-stories with 7 earthquake records with the effect of the length of the link

beam will be examined. Using this system, the considered structures are seismically reinforced and their performance with non-reinforced structures is evaluated. In this research, the possible configuration of seismic reinforcement system for reinforced concrete buildings is investigated. And 6 specimens considering the reference specimen and compressive strength of 250 kg/cm^2 , so with the aim of weakening the concrete frame with a compressive strength of 150 kg/cm^2 has been used. Table 1 indicates the specifications of studied specimens.

Table 1. The specifications of studied specimens

Specimen	Total height	Length of beam link	Compressive strength of concrete(kg/cm^2)	No. story
F6-MRF-C25-VL50CM	$6 \times 3 = 18\text{m}$	50cm	250	6
F6-MRF-C25-VL80CM	$6 \times 3 = 18\text{m}$	80cm	250	6
F6-MRF-C25-VL100CM	$6 \times 3 = 18\text{m}$	100cm	250	6
F12-MRF-C25-VL50CM	$12 \times 3 = 36\text{m}$	50cm	250	12
F12-MRF-C25-VL80CM	$12 \times 3 = 36\text{m}$	80cm	250	12
F12-MRF-C25-VL100CM	$12 \times 3 = 36\text{m}$	100cm	250	12
F6-MRF-C15-VL50CM	$6 \times 3 = 18\text{m}$	50cm	150	6
F6-MRF-C15-VL80CM	$6 \times 3 = 18\text{m}$	80cm	150	6
F6-MRF-C15-VL100CM	$6 \times 3 = 18\text{m}$	100cm	150	6
F12-MRF-C15-VL50CM	$12 \times 3 = 36\text{m}$	50cm	150	12
F12-MRF-C15-VL80CM	$12 \times 3 = 36\text{m}$	80cm	150	12
F12-MRF-C15-VL100CM	$12 \times 3 = 36\text{m}$	100cm	150	12

In the following, the most important purpose of numerical modeling of physical problems by different software is to obtain the behavior and response of the problem to the prevailing conditions. The studied specimens include 6-story and 12-story RC frames with a height of 3 m per floor and a total height of 18 m and 36 m, which are modelled in 6 specimens. The required material is provided and modeling and analysis will be done accordingly. Schematics and geometry of the models are given below. Johnson-cook theory is used for the properties of steel plastics. Johnson Cook's criterion is used to predict the onset of damage in soft metals based on Table 2. This model considers the plastic strain equivalent to the onset of injury as a function of the three-axis stress ratio and strain rate based on Table 3. It should be noted that the theory of Johnson Cook's criterion is available in the software documentation.

Table 2. Johnson-cook criterion

A	B	n	m	Melting Temp	Transition Temp
2.63E+08	1.30e+08	0.0915	1	1700	1300

Table 3. The values of strain rate

C	Epsilon dot Zero
0/022	1

The compressive strength of concrete is 150 kg/cm^2 for weakened specimens for improvement and the compressive strength of concrete is 250 kg/cm^2 for reference. The parameters of the *CDP* behavioral model, compressive behavior and compressive damage of concrete, tensile behavior values are given based on Tables 4 to 9. Also, the configuration of specimens such as *6* and *12*-stories are presented based on Figs 8 and 9.

Table 4. The parameters of CDP of concrete 150 kg/cm^2

Dilation Angle	Eccentricity	fb0/fc0	k	Viscosity
35	0.1	1.16	0.667	0.001

Table 5. The Compressive behaviour and compressive damage of concrete 150 kg/cm^2

Compressive (CDP)		Compressive Damage	
Stress (MPa)	in-strain	damage	in-strain
9000000	0	0	0
16793967	3.05E-05	0.013483	3.05E-05
22523018	0.000102	0.032991	0.000102
26666251	0.000237	0.062674	0.000237
29091278	0.00044	0.102243	0.00044
30000000	0.000764	0.160883	0.000764
28129409	0.001234	0.248201	0.001234
18990847	0.002784	0.524516	0.002784
16376674	0.003283	0.601383	0.003283
14156450	0.003767	0.666932	0.003767
12295341	0.004236	0.721662	0.004236
10741068	0.004693	0.766801	0.004693
9441310	0.00514	0.803811	0.00514
8349983	0.005579	0.834106	0.005579
7428670	0.006011	0.858937	0.006011
6646157	0.006437	0.879354	0.006437
5977358	0.006859	0.896214	0.006859
5402191	0.007277	0.910209	0.007277
4904560	0.007692	0.921889	0.007692
4471529	0.008104	0.931691	0.008104
4092648	0.008515	0.939963	0.008515
3759433	0.008923	0.946982	0.008923
3464957	0.00933	0.952971	0.00933
3203526	0.009736	0.958106	0.009736
2970438	0.01014	0.962531	0.01014

Compressive (CDP)		Compressive Damage	
Stress (MPa)	in-strain	damage	in-strain
2761782	0.010544	0.966363	0.010544
2574292	0.010946	0.969696	0.010946
2405221	0.011348	0.972607	0.011348
2252251	0.011749	0.97516	0.011749
2113412	0.01215	0.977408	0.01215
1987025	0.01255	0.979394	0.01255
1871650	0.01295	0.981156	0.01295
1766049	0.013349	0.982724	0.013349
1669152	0.013748	0.984123	0.013748
1580031	0.014147	0.985376	0.014147
1497877	0.014545	0.9865	0.014545
1421983	0.014944	0.987513	0.014944

Table 6. The values of tensile behaviour of concrete 150 kg/cm²

Tensile (CDP)		Tensile Damage	
Stress(MPa)	in-strain	damage	in-strain
3450652	0	0	0
1382097	0.0013	0.955019	0.0013

Table 7. The parameters of CDP of concrete 250 kg/cm²

Dilation Angle	Eccentricity	fb ₀ /fc ₀	k	Viscosity
35	0.1	1.16	0.667	0.001

Table 8. The Compressive behaviour and compressive damage of concrete 250 kg/cm²

Compressive (CDP)		Compressive Damage	
Stress (MPa)	in-strain	damage	in-strain
7500000	0	0	0
15211380	5.27E-05	0.023846	5.27E-05
19864489	0.000155	0.052047	0.000155
22934534	0.000324	0.090591	0.000324
24542121	0.000556	0.137647	0.000556
25000000	0.000837	0.191011	0.000837
23325732	0.001475	0.308361	0.001475
20613051	0.002157	0.424554	0.002157
17881111	0.00284	0.528242	0.00284
15474205	0.003509	0.615192	0.003509
13451856	0.004162	0.685644	0.004162

11777986	0.0048	0.741793	0.0048
10394306	0.005425	0.786303	0.005425
9245009	0.00604	0.82163	0.00604
8283325	0.006648	0.849809	0.006648
7471928	0.007249	0.872446	0.007249
6781553	0.007845	0.890778	0.007845
6189350	0.008437	0.90575	0.008437
5677440	0.009025	0.918081	0.009025
5231748	0.009611	0.928321	0.009611
4841116	0.010194	0.93689	0.010194
4496629	0.010775	0.944116	0.010775
4191103	0.011355	0.95025	0.011355
3918706	0.011933	0.955493	0.011933
3674662	0.01251	0.960002	0.01251
3455037	0.013086	0.963902	0.013086
3256562	0.013661	0.967293	0.013661
3076503	0.014235	0.970257	0.014235
2912564	0.014809	0.97286	0.014809
2762799	0.015382	0.975156	0.015382
2625553	0.015954	0.97719	0.015954
2499411	0.016526	0.978998	0.016526
2383153	0.017098	0.980613	0.017098
2275730	0.017669	0.982059	0.017669
2176228	0.01824	0.983358	0.01824
2083852	0.01881	0.984529	0.01881
1997906	0.019381	0.985588	0.019381
1917780	0.019951	0.986549	0.019951
1842936	0.02052	0.987421	0.02052

Table 9. The values of tensile behaviour of concrete 250 kg/cm²

Stress (MPa)	Tensile (CDP)		Tensile Damage	
	in-strain	damage	in-strain	damage
3150000	0	0	0	0
1249964	0.001298	0.956457	0.001298	0.956457

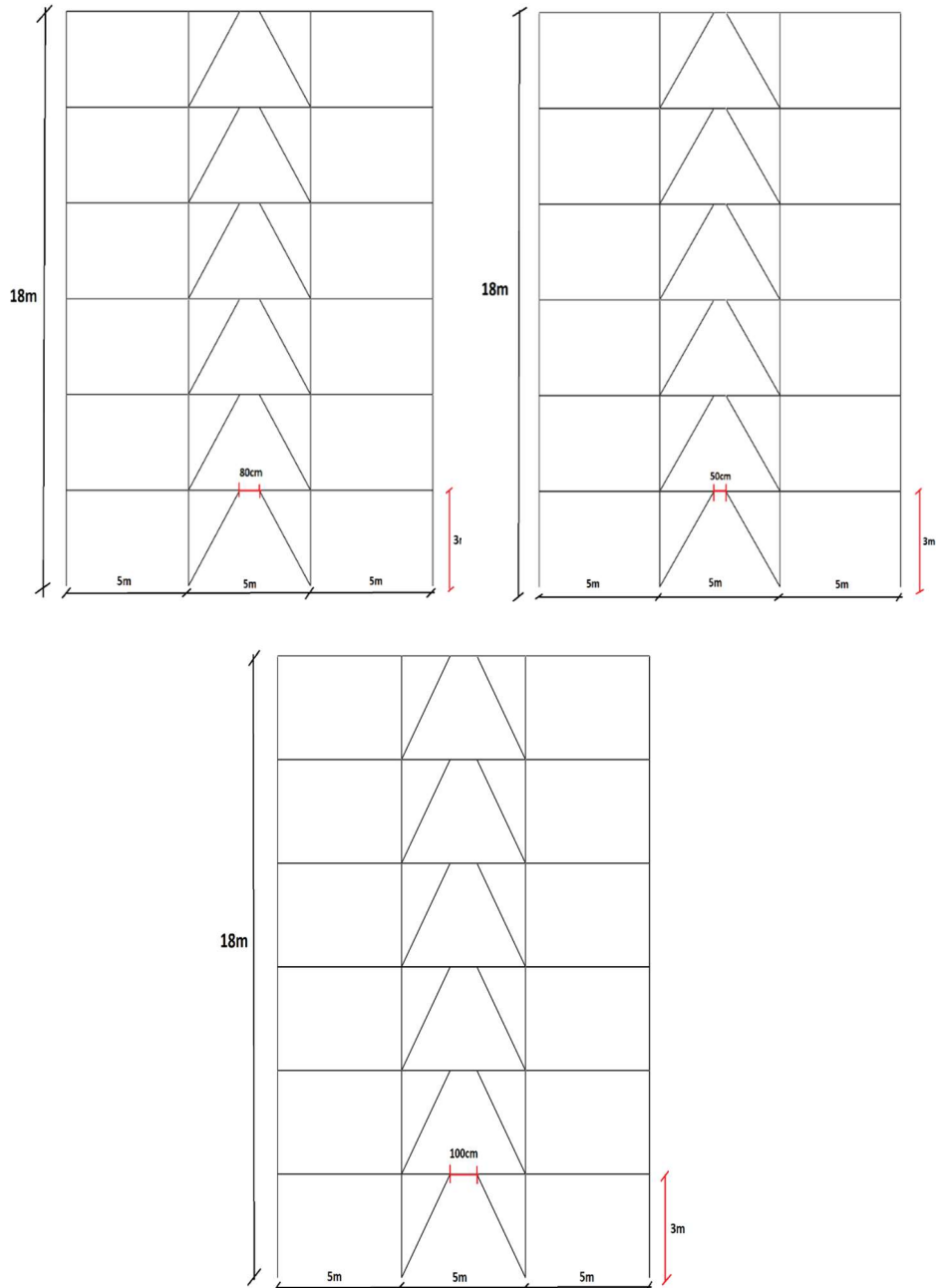


Fig. 8. 6-story frame with 50, 80 and 100 cm link beam length

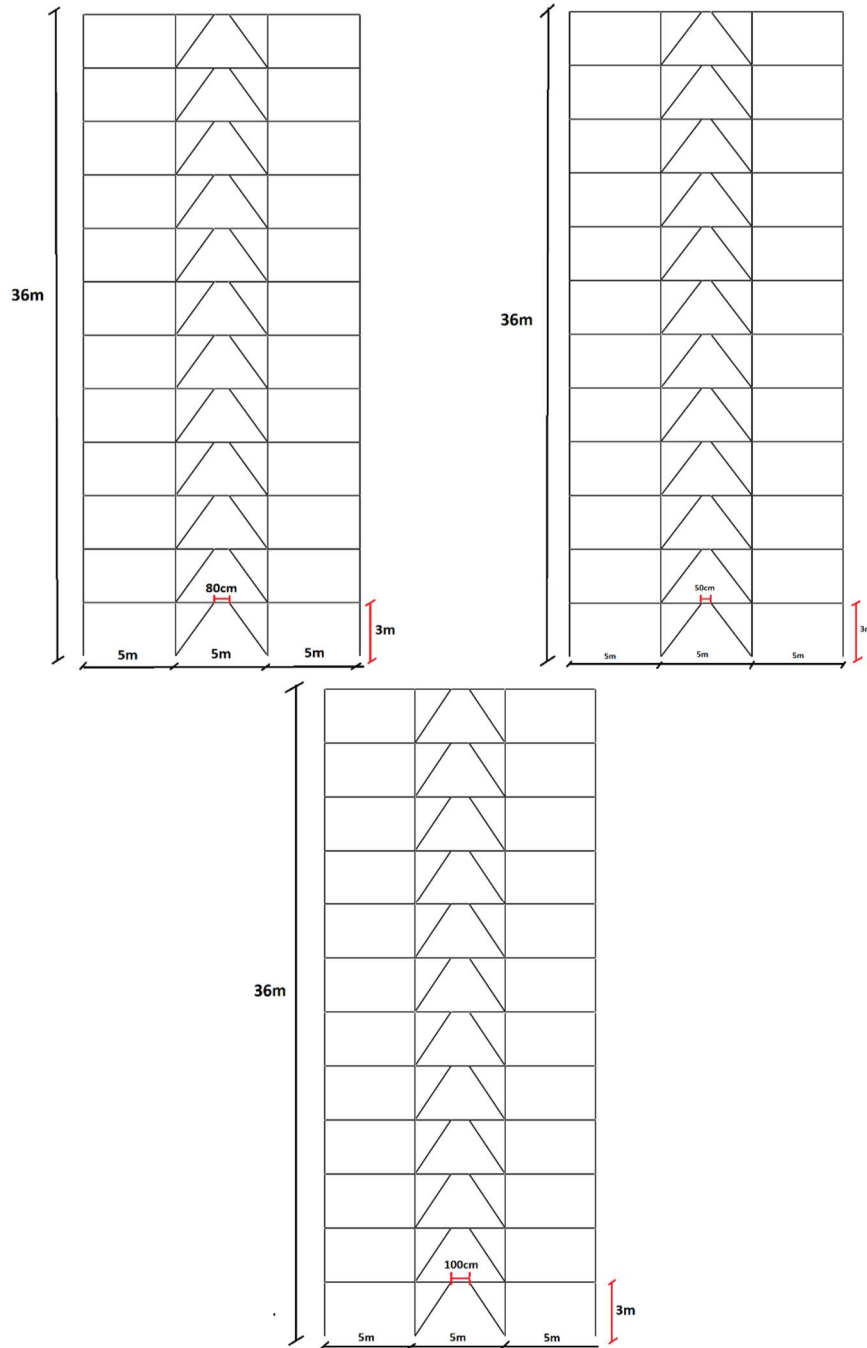


Fig. 9. 12-story frame with 50, 80 and 100 cm link beam length

2.3. The studied earthquake records

As previously stated, the main goal of this research was to evaluate the performance of eccentric brace placed in *RC* frame under near-field earthquakes. A single big long-period pulse of motion may be seen in the time history of the velocity record, which is one of the most essential features of near-field ground motion recorders. The forward directivity effect causes this characteristic of the velocity record. The majority of research that has looked at the influence of near field recordings has linked the damaging effects of a near field earthquake on buildings to this pulse-like characteristic. The influence of near field earthquakes on *RC* buildings rehabilitated with an eccentric brace with 6 and 12-stories was examined in this paper, regardless of the geotechnical factors leading in near field ground motion parameters. To accomplish this aim, the building performance was studied and compared for 7 near-fault earthquake records. The specifications of records are presented in Table 10.

Table 10. The specifications of records

ID	Earthquake	Year	M	Distance (km)	Soil	Fault	PGA (g)
1	Managua	1972	6.1	7	D	Thrust	0.52
2	Kobe	1995	7.3	14	D	Strike-slip	0.62
3	IMPVALL	1978	6.5	10	D	Strike-slip	0.44
4	super	1980	6.9	9	D	Strike-slip	0.50
5	bam	2003	6.6	7	D	Strike-slip	0.40
6	park	1991	6.8	10	D	Thrust	0.55
7	Darfield	2010	7.1	8	D	Thrust	0.49

3. RESULTS

3.1. 6-story frame

Due to the compatibility of eccentric braces with architectural conditions, their use is very common in ordinary buildings. According to the results obtained due to the effect of link beam in an eccentric brace on seismic improvement in weak *RC* frames, 7 near-fault records are selected to perform nonlinear dynamic time history analyses. When the link beam is affected by the shear and flexural forces of its plastic, it deforms and rotates relative to its original position. According to the obtained curves and software results, the behavior of long length link beam under heavy periodic loading is generally weak compared to short length link beam and the result is low stiffness, strength and energy dissipation capacity. Therefore, for the correct behavior of the eccentric bracing frame system, the use of short link beam with shear yield is recommended. By examining 7 near-fault

records and the length of the beam of 50, 80 and 100 cm, the displacement of the specimen on a curve for a better comparison with the specimen modelled with concrete has a higher compressive strength of 250 cm. In the following, the applied record to the 6-story frame based on Fig. 10. The displacement time history curves are presented for RC frame rehabilitated with an eccentric brace with different length of link beam under 7 near fault records based on Figs 11 to 13. Meanwhile, the base shear time history curves are presented for RC frame rehabilitated with an eccentric brace with different length of link beam under 7 near fault records based on Figs 14 to 16.

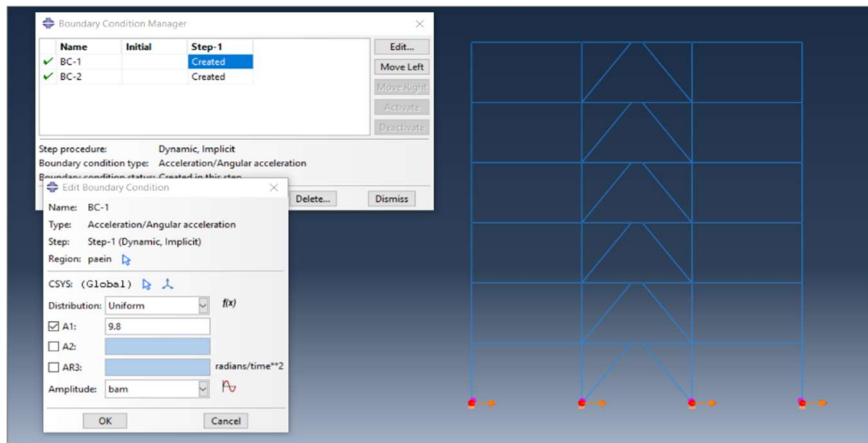


Fig. 10. The applied record to the 6-story frame

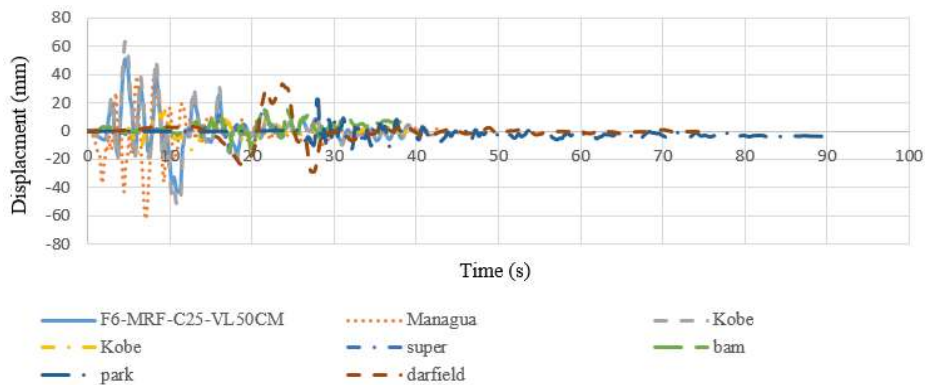


Fig. 11. Comparison of displacement-time curve of specimens with 50 cm link beam length and specimen F6-MRF-C25-VL50CM

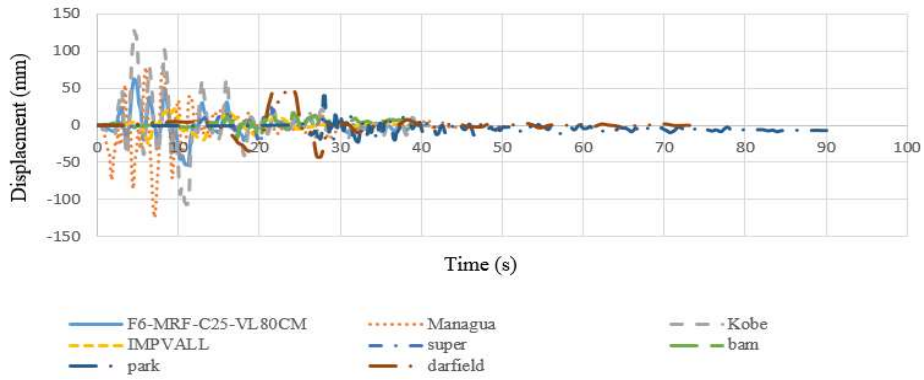


Fig. 12. Comparison of displacement-time curve of specimens with 80 cm link beam length and specimen F6-MRF-C25-VL80CM

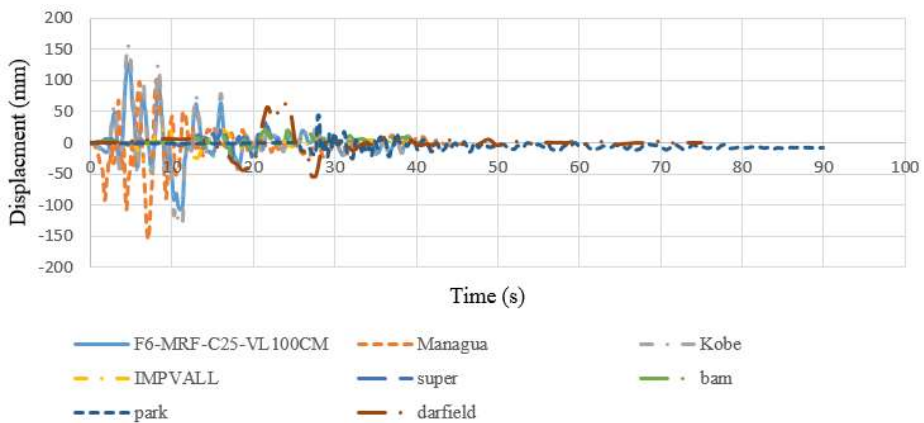


Fig. 13. Comparison of displacement-time curve of specimens with 100 cm link beam length and specimen F6-MRF-C25-VL100CM

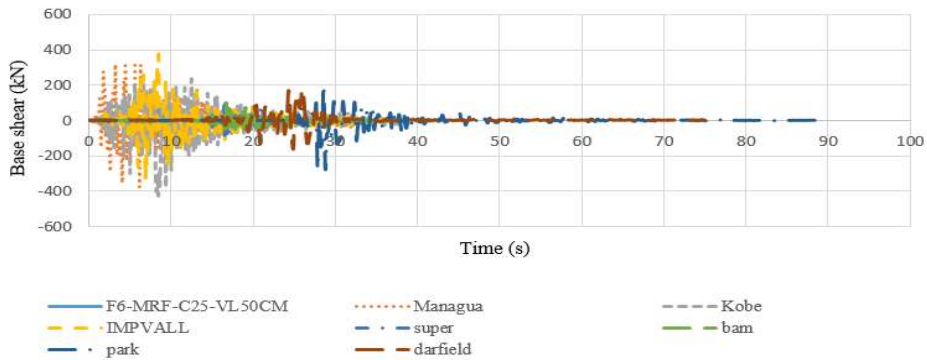


Fig. 14. Comparison of base shear-time curve of specimens with 50 cm link beam length and specimen F6-MRF-C25-VL50CM

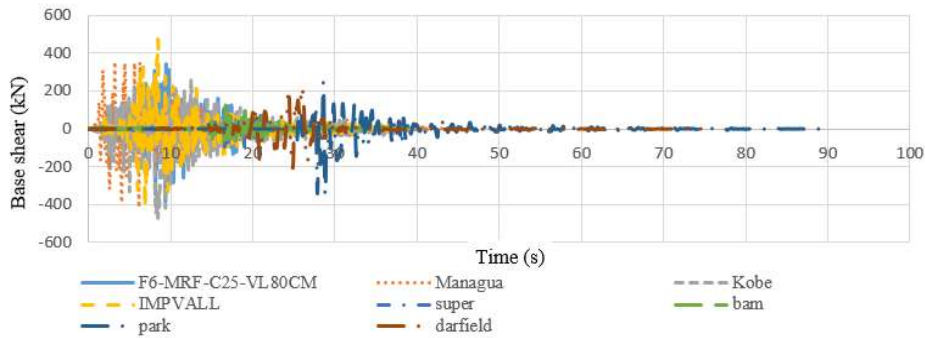


Fig. 15. Comparison of base shear-time curve of specimens with 80 cm link beam length and specimen F6-MRF-C25-VL80CM

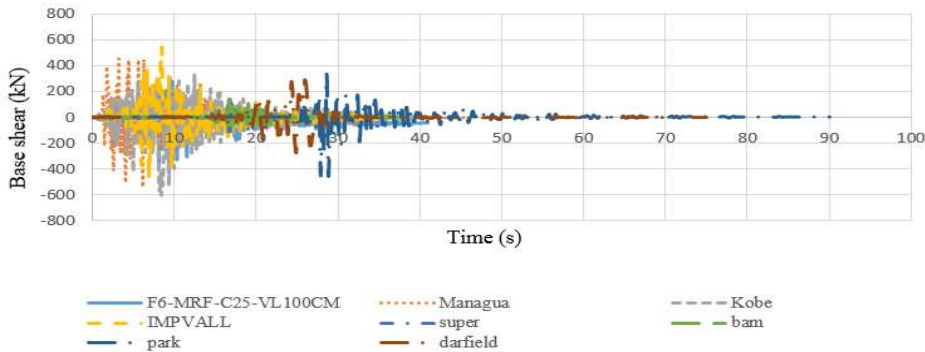


Fig. 16. Comparison of base shear-time curve of specimens with 100 cm link beam length and specimen F6-MRF-C25-VL100CM

Short-link beams performance are far better than long-link beams, and short-link beams provide more energy loss and more ductility; Therefore, in the design of the link beam, the shear of the link beam is mainly considered as a ductile component because, as it is mentioned, the link beam is a control deformation member. The axial force in the beam (which is due to the application of lateral load to the structure) reduces both the bending capacity and the shear capacity of the link beam and also reduces the capacity of inelastic deformation of the link beam. The evaluation of displacement and base shear values in *F6-MRF-C15-VL50CM*, *F6-MRF-C15-VL80CM* and *F6-MRF-C15-VL100CM* under 7 records are presented based on Table 11.

Table 11. Evaluation of displacement and base shear values in F6-MRF-C15-VL50CM, F6-MRF-C15-VL80CM and F6-MRF-C15-VL100CM under 7 records

6-story		F6-MRF-C15-VL50CM		F6-MRF-C15-VL80CM		F6-MRF-C15-VL100CM	
Earthquake	M _w	Displacement (mm)	Base shear (kN)	Displacement (mm)	Base shear (kN)	Displacement (mm)	Base shear (kN)
Managua	6.1	40.73	320	81.46	355.57	99.93	457.16
Kobe	7.3	62.38	227.69	121.91	252.99	152.39	352.27
IMPVALL	6.5	14.57	372.87	21.85	466.09	24.64	532.68
super	6.9	17.46	98.68	26.20	123.27	29.18	138.41
bam	6.6	17.46	98.62	19.24	123.27	22.74	140.88
park	6.8	21.81	198.54	39.27	248.17	43.63	330.90
Darfield	7.1	21.8112	198.54	49.26	218.92	64.03	291.89

3.2. 12-story frame

Steel braces are often used to rehabilitate *RC* buildings. According to the results obtained, the behavior of long length link beam under seismic loading is generally weak compared to short length link beam and the result is low stiffness, strength and energy dissipation capacity. Therefore, for the correct behavior of the eccentric bracing frame system, the use of short link beams with shear yield is recommended. In the following, the applied record to the 12-story frame based on Fig. 17. The displacement time history curves are presented for *RC* frame rehabilitated with an eccentric brace with different length of link beam under 7 near fault records based on Figs 18 to 20.

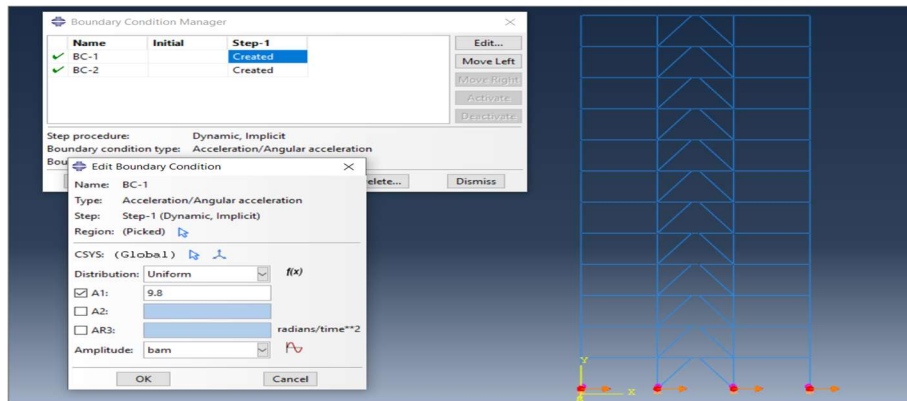


Fig. 17. The applied record to the 12-story frame

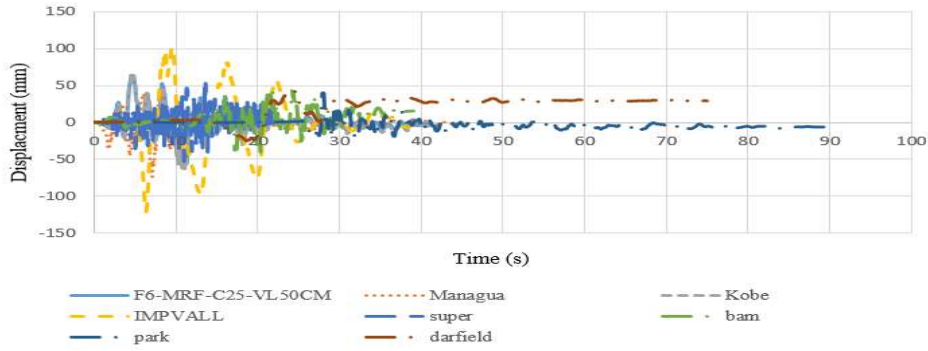


Fig. 18. Comparison of displacement-time curve of specimens with 50 cm link beam length and specimen F12-MRF-C25-VL50CM

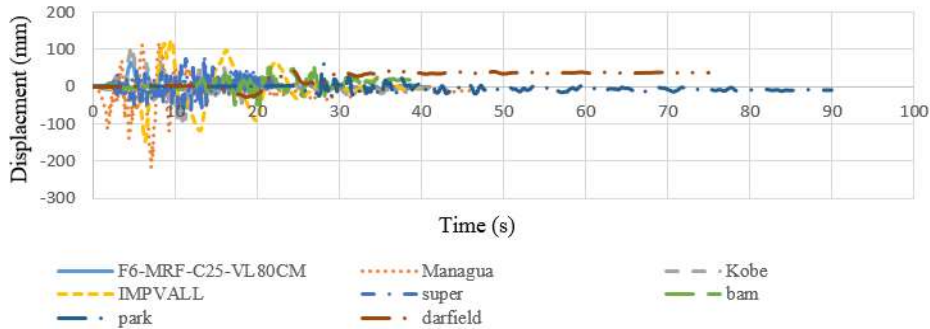


Fig. 19. Comparison of displacement-time curve of specimens with 80 cm link beam length and specimen F12-MRF-C25-VL80CM

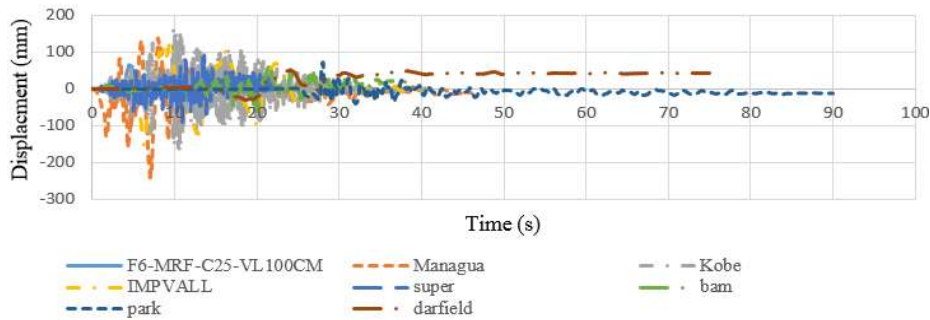


Fig. 20. Comparison of displacement-time curve of specimens with 100 cm link beam length and specimen F12-MRF-C25-VL100CM

Meanwhile, the base shear time history curves are presented for RC frame rehabilitated with an eccentric brace with different lengths of link beam under 7 near-fault records based on Figs 21 to 23.

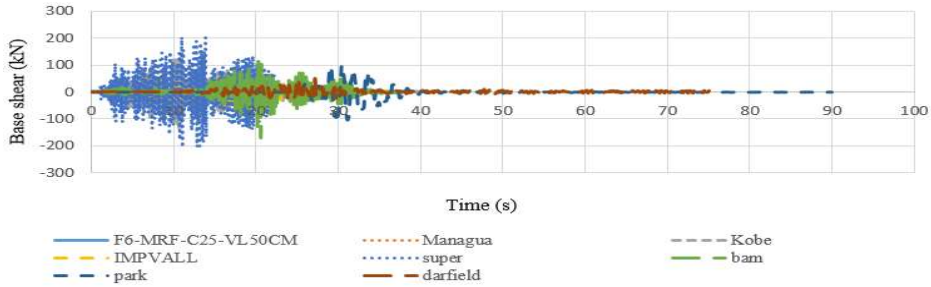


Fig. 21. Comparison of base shear-time curve of specimens with 50 cm link beam length and specimen F12-MRF-C25-VL50CM

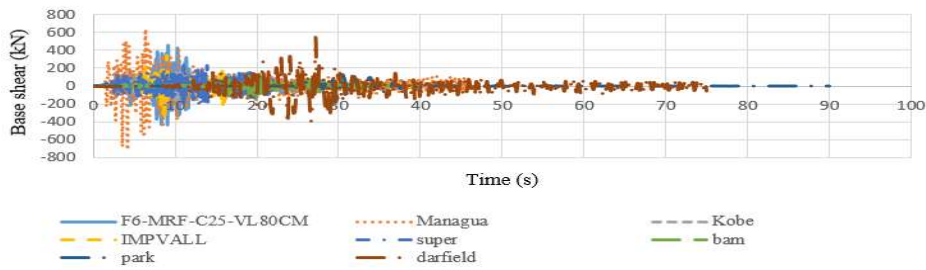


Fig. 22. Comparison of base shear-time curve of specimens with 80 cm link beam length and specimen F12-MRF-C25-VL80CM

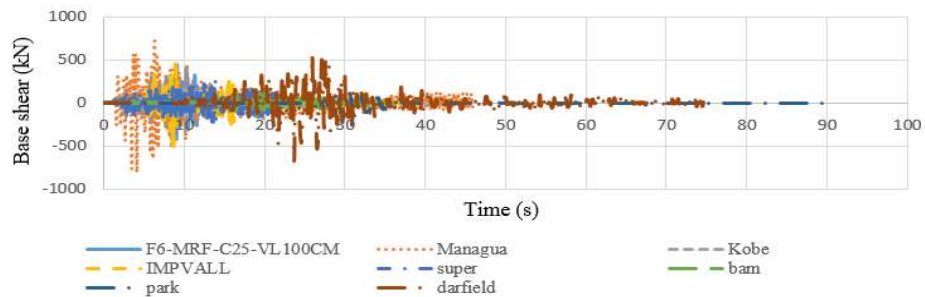


Fig. 23. Comparison of base shear-time curve of specimens with 100 cm link beam length and specimen F12-MRF-C25-VL100CM

The evaluation of displacement and base shear values in *F12-MRF-C15-VL50CM*, *F12-MRF-C15-VL80CM* and *F12-MRF-C15-VL100CM* under 7 records are presented based on Table 12.

Table 12. Evaluation of displacement and base shear values in F12-MRF-C15-VL50CM, F12-MRF-C15-VL80CM and F12-MRF-C15-VL100CM under 7 records

12-story		F12-MRF-C15-VL50CM	F12-MRF-C15-VL80CM	F12-MRF-C15-VL100CM		F12-MRF-C15-VL50CM	F12-MRF-C15-VL80CM	F12-MRF-C15-VL100CM
Earthquake	M _w	Displacement (mm)	Base shear (kN)	Displacement (mm)	Base shear (kN)	Displacement (mm)	Base shear (kN)	Base shear (kN)
Managua	6.1	55.70	622.39	66.21	615.04	70.33	702.91	
Kobe	7.3	63.80	125.80	99.28	163.55	107.39	165.20	
IMPVALL	6.5	101.18	93.01	116.97	339.97	129.25	509.96	
super	6.9	52.44	201.82	83.91	224.25	89.16	252.28	
bam	6.6	44.77	131.87	52.44	126.70	60.77	153.67	
park	6.8	39.05	100.29	65	125.37	69.72	143.28	
Darfield	7.1	43.78	496.75	37.86	550.55	41.31	556.09	

4. CONCLUSIONS

A building may need retrofitting for a variety of reasons, such as changes in building use, changes in design standards, or defects in the design and construction of the building. One of the methods used in recent years for seismic rehabilitation of reinforced concrete frames is to strengthen the structure by using steel braces. In this paper, by utilizing nonlinear dynamic analyses such as time history, the role of steel eccentric brace in seismic rehabilitation of weak reinforced concrete structures is determined and their seismic performance are compared with the reference model through the time history nonlinear dynamic analysis.

- During the seismic analyses, the displacement of the structure in the direction of accelerograms is reduced, which is certainly due to the presence of bracing, and as was quite expected, more stiffness that occurs with the presence of bracing reduces the displacement of the structure.

- On the other hand, by enhancing the stiffness and decreasing the overall ductility of the structure causes a relative increase in the base shear during the earthquake, according to the base shear-time diagrams. Also, the main structure remains in a linear state and only the link beam enters the nonlinear range.

- The shear behavior of the beam in this system and the absorption of energy due to plastic deformation has reduced the stress in the reinforced concrete frame, especially concrete, which shows the efficiency of the system in concrete structures. The noteworthy point in this part is the reduction of stress in concrete by reducing the length of link beam and increasing the capacity of the system.

- Another positive feature of the system is that the link beam prevents the buckling of the compressive brace. In fact, the system is designed so that the link beam yields before the buckling of the compressive brace. Then, the link beam reaches

the yield force of the cross section with a limited displacement, which is also presented in all shapes.

- Throughout the application of accelograms, the displacement of the structure in the direction of accelograms is reduced, which is certainly due to the presence of an eccentric bracing, and reduces the displacement of the structure.

- Short-link beams perform far better than long-link beams, and short-link beams provide more energy dissipation and more ductility; therefore, in the design of the link beam, the shear of the link beam is mainly considered as a ductile component. The axial force in the beam (which is due to the application of lateral load to the structure) reduces both the bending capacity and the shear capacity of the link beam and also reduces the capacity of inelastic deformation of the link beam.

REFERENCES

1. ASCE. SEI/ASCE 7-05. 2005. Minimum design loads for buildings and other structures. Washington DC: *American Society of Civil Engineers*.
2. Del Valle, E 1980. Some lessons from the March 14 earthquake in Mexico City. *Proceedings of the 7th world conf. on earthquake engrg.*
3. Miranda, E and Bertero, VV 1990. Post-tensioning technique for seismic upgrading of existing low-rise buildings. *Proceedings of the 4th US national conference on earthquake engineering*.
4. Badoux, M and Jirsa, JO 1990. Steel bracing of RC frames for seismic retrofitting. *J Struct Eng* **116** (1), 55–74.
5. Bush, TD Jones, EA and Jirsa, JO 1991. Behavior of RC frame strengthened using structural steel bracing. *J Struct Eng* **117** (4), 1115–26.
6. Rodriguez, M and Park, R 1991. Repair and strengthening of reinforced concrete buildings for seismic resistance. *Earthq Spectra* **7** (3), 439–59.
7. Pincheira, JA 1993. Design strategies for the seismic retrofit of reinforced concrete frames. *Earthq Spectra* **9** (4), 817–42.
8. Lobo, RF, Bracci, JM, Shen, KL, Reinhorn, AM and Soong, TT 1993. Inelastic response of R/C structures with viscoelastic braces. *Earthq Spectra* Vol. **9** (3), 419–46.
9. Nateghi, AF 1995. Seismic strengthening of eight storey RC apartment building using steel braces. *Eng Struct* **17** (6), 455–61.
10. Pincheira, JA and Jirsa, JO 1995. Seismic response of RC frames retrofitted with steel braces or walls. *J Struct Eng* **121** (8), 1225–35.
11. Masri, AC and Goel, SC 1996. Seismic design and testing of an RC slab-column frame strengthened by steel bracing. *Earthq Spectra* **12** (4), 645–66.
12. Ghobarah, A and Abou Elfath, H 2001. Rehabilitation of a reinforced concrete frame using eccentric steel bracing. *Eng Struct* **23** (7), 745–55.

13. Youssef, MA, Ghaffarzadeh, H and Nehdi, M 2007. Seismic performance of RC frames with concentric internal steel bracing. *Eng Struct* **29** (7), 1561–8.
14. Mazzolani, FM 2008. Innovative metal systems for seismic upgrading of RC structures. *J Constr Steel Res* **64** (7), 882–95.
15. Sadeghi, A, Kazemi, H and Samadi, M 2021. Reliability and Reliability-based Sensitivity Analyses of Steel Moment-Resisting Frame Structure subjected to Extreme Actions, *Frattura ed Integrità Strutturale* **15** (57), 138–159.
16. Sadeghi, A, Kazemi, H and Samadi, M 2021. Probabilistic seismic analysis of steel moment-resisting frame structure including a damaged column, *Structures* **33**, 187-200.
17. Tahamouli Roudsari, M, Entezari, A, Hadidi, MH and Gandomian, O 2017. Experimental Assessment of Retrofitted RC Frames with Different Steel Braces, *Structures* **11**, 206-217.
18. International Organization for Standardization (ISO). 2009. ISO 898-1, mechanical properties of fasteners made of carbon steel and alloy steel. Part 1: bolts, screws and studs with specified property classes — coarse thread and fine pitch thread. *Geneva, Switzerland*.
19. ACI 374 Committee, 374.1-05. 2006. Acceptance criteria for moment frames based on structural testing and commentary. Farmington Hills, Mich: *American Concrete Institute*.

Editor received the manuscript: 16.01.2022